European Journal of Medicinal Chemistry 123 (2016) 777–787

Contents lists available at ScienceDirect

European Journal of Medicinal Chemistry

journal homepage: http://www.elsevier.com/locate/ejmech

Research paper

Systemic optimization and structural evaluation of quinoline derivatives as transthyretin amyloidogenesis inhibitors

Boyoung Kim [a, 1], Hwanggue Park [a, 1], Seul Ki Lee [a], Sung Jean Park [b], Tae-Sung Koo [a], Nam Sook Kang [a], Ki Bum Hong [c, **], Sungwook Choi [a, *]

[a] Department of New Drug Discovery and Development, Chungnam National University, 99 Daehak-ro Yuseong-gu, Daejon, 305-764, Republic of Korea
[b] College of Pharmacy, Gachon University, 534-2 Yeonsu 3-dong, Yeonsu-gu, Incheon, 406-799, Republic of Korea
[c] New Drug Development Center (NDDC), Daegu-Gyeongbuk Medical Innovation Foundation (DGMIF), 80 Cheombok-ro, Dong-gu, Daegu, 701-310, Republic of Korea

ARTICLE INFO

Article history:
Received 31 May 2016
Received in revised form
2 August 2016
Accepted 4 August 2016
Available online 6 August 2016

Keywords:
Amyloid
Amyloidogenesis
Transthyretin
Quinoline
In silico docking study
Pharmacokinetic

ABSTRACT

Wild type transthyretin (TTR) and mutant TTR misfold and misassemble into a variety of extracellular insoluble amyloid fibril and/or amorphous aggregate, which are associated with a variety of human amyloid diseases. To develop potent TTR amyloidogenesis inhibitors, we have designed and synthesized a focused library of quinoline derivatives by Pd-catalyzed coupling reaction and by the Horner–Wadsworth–Emmons reaction. The resulting 2-alkynylquinoline derivatives, (*E*)-2-alkenylquinoline derivatives, and (*E*)-3-alkenylquinoline derivatives were evaluated to inhibit TTR amyloidogenesis by utilizing the acid-mediated TTR fibril formation. Among these quinoline derivatives, compound **14c** exhibited the most potent *anti*-TTR fibril formation activity in the screening studies, with IC_{50} values of 1.49 μM against WT-TTR and 1.63 μM against more amyloidogenic V30 M TTR mutant. That is comparable to that of approved therapeutic drug, tafamidis, to ameliorate transthyretin-related amyloidosis. Furthermore, rationalization of the increased efficacy of compound **14c** bearing a hydrophobic substituent, such as chloride, was carried out by utilizing *in silico* docking study that could focus on the region of the thyroid hormone thyroxine (T_4) binding sites. Additionally, the most potent compound **14c** exhibited good pharmacokinetics properties. Taken together, the novel quinoline derivatives could potentially be explored as potential drug candidates to treat the human TTR amyloidosis.

1. Introduction

Human amyloid diseases such as Alzeheimer's disease, Parkinson's disease, type II diabetes, light chain amyloidosis, and transthyretin amyloidosis are characterized by aberrant protein misfolding, misassembly, and deposition in the fibrillary cross-β-sheet amyloid fibril [1–3]. Transthyretin (TTR) is one of more than 30 nonhomologous human amyloidogenic proteins and peptides [4–6]. Amyloidogenesis of wild type (WT) TTR or one of over 100 thermodynamically less stable mutants of TTR appears to elicit the proteotoxicity and cell degeneration, which cause senile systemic amyloidosis (SSA), familial amyloid polyneuropathy (FAP), familial amyloid cardiomyopathy (FAC), or central nervous system selective amyloidosis (CNSA). SSA is associated with WT-TTR deposition in the heart and a late onset disease that affects up to 20% of the aged population [3], whereas tissue selective deposition of one of less stable mutants of TTR and cell degeneration results in FAP (e.g., V30M-TTR), FAC (e.g., V122I-TTR), and CNSA (e.g., D18G and A25T-TTR) [5–11].

TTR is a homotetrameric protein composed of 127-amino-acid, β-sheet-rich subunits [12]. The established physiological functions of TTR are to bind to and transport the thyroid hormone thyroxine (T_4) and *holo*-retinol binding protein in the blood and cerebrospinal fluid (CSF) [5,13]. TTR has two unique dimer-dimer interface, creating two funnel-shaped thyroxine binding sites as shown in Fig. 1A [14]. Because there are two major thyroxine carriers such as albumin and thyroid-binding globulin in the blood, more than 99% of thyroxine binding sites within TTR tetramer are unoccupied [5]. TTR fibril formation requires the rate-limiting tetramer dissociation

* Corresponding author.
** Corresponding author.
E-mail addresses: kbhong@dgmif.re.kr (K.B. Hong), swchoi2010@cnu.ac.kr (S. Choi).
[1] These authors contributed equally to this work.

http://dx.doi.org/10.1016/j.ejmech.2016.08.003
0223-5234/

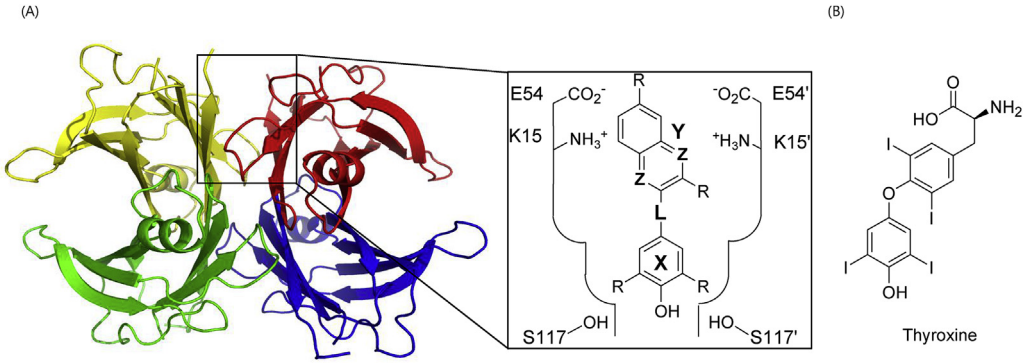

Fig. 1. (A) The X-ray crystal structure (PDB 2ROX) of WT-TTR with expanded view of one of thyroxine binding sites and proposed binding mode of small molecules. (B) Chemical structure of thyroxine.

and misassembly of partially denatured monomeric subunits into insoluble amyloid fibril and/or amorphous aggregate [5,15,16]. Reversible and irreversible small molecules that bind to one or two of thyroxine binding sites stabilize the ground state of tetrameric TTR and raise the kinetic barrier for dissociation, resulting in kinetic stabilization on TTR and preventing aggregation [5,17–37].

Oral tafamidis (Vyndaqel®) is only one approved therapeutic drug to ameliorate transthyretin-related amyloidosis. Tafamidis was initially used in Europe in 2011 for adult patients with early stage symptomatic polyneuropathy and has since been approved in Argentina, Japan, and Mexico for the treatment of TTR familial amyloid polyneuropathy (TTR-FAP). The drug selectively binds to thyroxine binding sites within TTR tetramer with negative cooperativity and kinetically stabilize the WT-TTR and the variant TTR tetramer through prevention of TTR dissociation, the rate-limiting step of TTR amyloid fibril formation [38–40]. In this study, numerous structure-activity relationship studies were carried out to identify TTR amyloidogenesis inhibitors with desirable pharmacological properties: aromatic X ring bearing polar substituents for hydrogen bond interaction with the Ser-117 or Thr-119 hydroxyl groups and van der Waals interaction in the inner binding cavity, hydrophobic linker L, and aromatic Y ring bearing polar substituents for electrostatic and/or hydrogen bond interactions with the Lys 15 and/or the Glu-54 in the outer binding cavity (Fig. 1B). On the basis of previous structural data [17,18,22–30,32,34,36], we chose focused substituents on the two aromatic rings (X and Y) and two kinds of linker to design potent WT- and V30M-TTR amyloidogenesis inhibitors and compared their potency to that of tafamidis. We investigated the molecular mechanism for the *anti*-TTR fibril formation activity of quinoline derivatives by performing *in silico* docking studies and reported the PK evaluations of two potent inhibitors *in vivo*.

2. Results and discussion

2.1. Chemistry

The general procedure for the synthesis of 2-alkynylquinoline derivatives **7a-i** was outlined in Scheme 1. Intermediates **2a**-**e**, obtained by the protection of hydroxyl group with MEM group or TIPS group, were treated with TMS-acetylene under Pd/Cu catalyzed Sonogashira coupling conditions to afford TMS-protected alkynes **3a**-**e** in 40%–94% yield. TMS-deprotected alkynes **4a**-**e**, which were prepared from deprotection of TMS group with K_2CO_3 in MeOH, were coupled with 2-chloroquinoline derivatives **5a-d** via a second Pd/Cu catalyzed Sonogashira coupling reactions. The final 2-alkynylquinoline derivatives **7a-h** were conveniently obtained by the deprotection of MEM or TIPS groups and 2-alkynylquinoline derivatives **7h** was subjected to reduction with Sn powder in AcOH and HCl to give 2-alkynylquinoline derivatives **7i**.

The Heck coupling reaction of 2-chloroquinoline derivatives **5a** and **5d** and terminal alkene **8** [34] in the presence of $Pd_2(dba)_3$, a variety of ligands (P(*o*-Tol)$_3$, PPh_3, *t*ButylXPhos), and a variety of bases (Et_3N, K_2CO_3, Cy_2NMe) was utilized as shown in Scheme 2. Among them, *N,N*-Dicyclohexylmethylamine (Cy_2NMe) and *t*ButylXPhos were found to be very effective additives to give (*E*)-2-alkenylquinoline derivatives **9a** and **9b**. Deprotection of MEM groups of **9a** and **9b** using concentrated HCl afforded the corresponding (*E*)-2-alkenylquinoline derivatives **10a** and **10b** and subsequently, the nitro compound **10b** was treated with $SnCl_2 \cdot 2H_2O$ in EtOH to produce the amine compound **10c**.

Finally, the (*E*)-3-alkenylquinoline derivatives **14a** and **14b** were prepared by the Horner–Wadsworth–Emmons reactions between substituted 2-chloroquinoline-carbaldehydes **11a** and **11b** and diethyl phosphonate **12** [37] followed by the deprotection of MEM groups using concentrated HCl as shown in Scheme 3. Subsequently, the demethylation of **14b** with BBr_3 provided (*E*)-3-alkenylquinoline derivatives **14c**.

2.2. Biological evaluation

2.2.1. Inhibition of WT- and V30M-TTR amyloidogenesis by quinoline derivatives

The newly synthesized quinoline derivatives are evaluated their ability to inhibit TTR amyloidogenesis using the previously established acid-mediated TTR fibril formation assay [41]. Briefly, a candidate inhibitor (3.6 or 7.2 μM) was preincubated with a physiological concentration of WT-TTR or V30M-TTR (each 3.6 μM) and amyloidogenesis was triggered by adjusting the pH to 4.4. The turbidity of the sample solution was measured after 72 h incubation at 37 °C to evaluate their ability to prevent WT-TTR or V30M-TTR amyloidogenesis. The potency of candidate inhibitors was expressed as the percentage of TTR fibril formation, compared to TTR fibril formation in the absence of inhibitor, as shown in Tables 1–3.

The first study was focused on the effect of a variety of hydrophobic substituents flanked by 4-hydroxyl group on an aryl-X ring. It is clear that the hydrophobic group such as methyl group play a critical role in enhancing binding potency (**7a** vs **7b**). However, the decrease in potency of compounds **7c**-**e** with bigger hydrophobic groups over compound **7b** suggests that the small hydrophobic group is essential for WT-TTR binding, due to spatial limitation in the inner binding cavity. We then shift our attention to the effect of substituents on a quinoline-Y ring, while holding the 3,5-dimethyl-

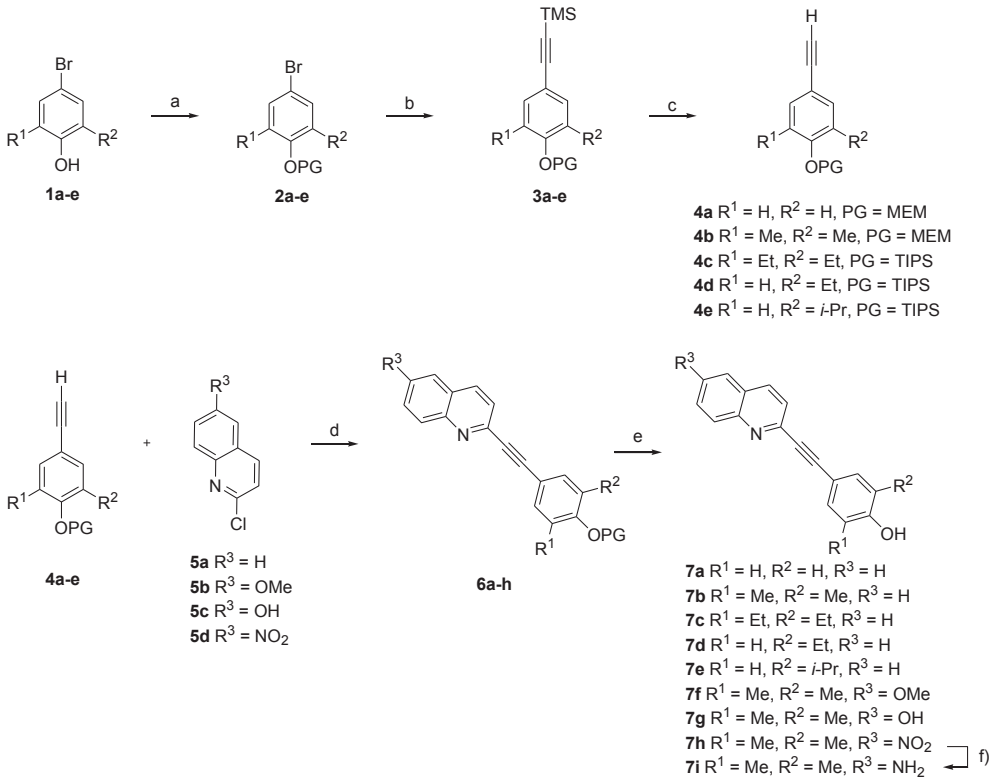

Scheme 1. Reagents and conditions a) NaH, TIPSCl, 3–14 h for **2a** and **2b** or NaH, MEMCl, THF, 18 h for **4c**-**e**; b) Ethynyltrimethylsilane, $Pd(PPh_3)_2Cl_2$, CuI, Et_3N, MeCN, 66 °C, 3–17 h; c) K_2CO_3, MeOH, 1.5–8 h; d) $Pd(PPh_3)_2Cl_2$, CuI, Et_3N 3–7 h, 80 °C; e) conc.HCl, THF/MeOH = 1:1 (v/v), r.t., 4–20 h for **7a**, **7b**, **7f**, **7g** or 1 M TBAF, THF, 1–2.5 h, for **7c**-**e**, **7h** ; f) Sn powder, AcOH, HCl, r.t., 1 h for **7i**.

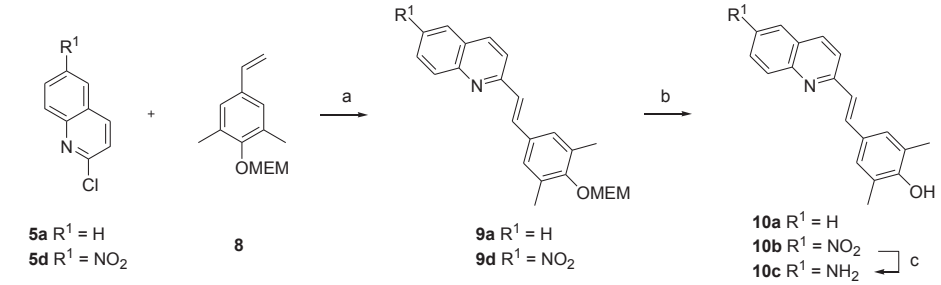

Scheme 2. Reagents and conditions a) $Pd_2(dba)_3$, *t*ButylXPhous, Cy_2NMe, Dioxane, 120 °C, 18–40 h; b) conc.HCl, THF/MeOH = 1:1 (v/v), r.t.,6–20 h; c) $SnCl_2$ $2H_2O$, EtOH, r.t., 9 h.

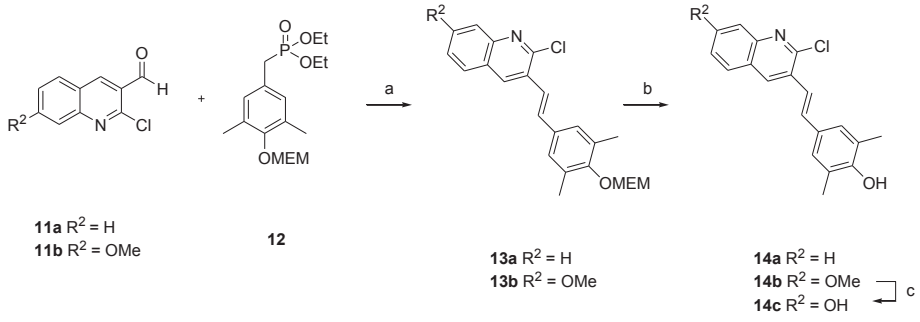

Scheme 3. Reagents and conditions a) *t*BuOK, DMF, 60 °C, 1–6 h; b) conc.HCl, THF/MeOH = 1:1 (v/v), r.t., 5–20 h; c) BBr_3, DCM, −78 °C to r.t., 22 h.

4-hydroxy-substituted aryl-X ring constant. This series with relative hydrophilic substituents displayed increased levels of potency compared to the unsubstituted lead compound **7b**, except compound **7f** with a hydrophobic methoxy group on the quinoline-Y ring.

In order to induce further structural optimization, we asked

Table 1
Inhibition of WT-TTR amyloid fibril formation under acidic denaturation condition in the presence of quinoline derivatives.

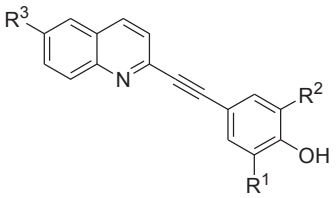

Compound	R^1	R^2	R^3	% Fibril Formation (WT-TTR)[a]		IC_{50} (μM)
				7.2 μM	3.6 μM	
7a	H	H	H	73.9%	–	–
7b	Me	Me	H	10.2%	25.6%	2.18
7c	Et	Et	H	93.4%	–	–
7d	H	Et	H	99.0%	–	–
7e	H	i-Pr	H	97.3%	–	–
7f	Me	Me	OMe	22.1%	–	–
7g	Me	Me	OH	9.6%	32.1%	2.59
7h	Me	Me	NO_2	3.6%	20.9%	2.06
7i	Me	Me	NH_2	4.8%	17.9%	1.90

[a] % Fibril formation represents the extent of WT-TTR fibril formation in the presence of inhibitors (7.2 M μM or 3.6 μM inhibitor, 3.6 μM WT-TTR, pH 4.4, 37 °C, 72 h), compared to untreated WT-TTR (100% fibril formation).

whether we could substitute the acetylene linker in the context of an aryl-quinoline scaffold composed of 3,5-dimethyl-4-hydroxy-substituted aromatic X ring and one aromatic Y ring bearing different substituents. While a detrimental effect in potency was observed with the simple replacement of the acetylene linker to the ethylene linker (**10a-c**), addition of a hydrophobic substituent such as a chloride group on the quinoline-Y ring dramatically increased the efficacy (**14c**, IC_{50} value of 1.49 μM), which is comparable to that observed with tafamidis (IC_{50} value of 1.55 μM). It is likely that the chloride substituents extend into the two symmetry-related halogen binding pockets (HBP) 1 and 1'.

Table 3
Inhibition of more amyloidogenic V30M-TTR amyloid fibril formation under acidic denaturation condition in the presence of tafamidis and quinoline derivative **14c**.4

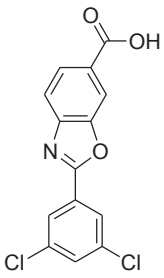

Tafamidis

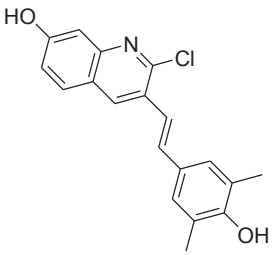

14c

Compound	% Fibril Formation (V30M-TTR)[a]		IC_{50} (μM)
	7.2 μM	3.6 μM	
Tafamidis	3.2%	17.0%	1.62
14c	5.0%	16.6%	1.63

[a] % Fibril formation represents the extent of more amyloidogenic V30M-TTR fibril formation in the presence of inhibitors (7.2 μM or 3.6 μM inhibitor, 3.6 μM V30M-TTR, pH 4.4, 37 °C, 72 h), compared to untreated V30M-TTR (100% fibril formation).

Furthermore, the most potent compound **14c** was reevaluated against one of the most clinically significant mutant TTR (V30M-TTR) as shown in Table 3. Importantly, compound **14c** allowed 5% of V30M-TTR fibril formation at a concentration of 7.2 μM and 16.6% of V30M-TTR fibril formation at a concentration equal to the V30M-TTR tetramer (3.6 μM). Dose-dependent fibril formation inhibition demonstrated that compound **14c**, with IC_{50} value of 1.63 μM, exhibited similar potency to tafamidis with IC_{50} value of 1.62 μM.

Table 2
Inhibition of WT-TTR amyloid fibril formation under acidic denaturation condition in the presence of tafamidis and quinoline derivatives.3

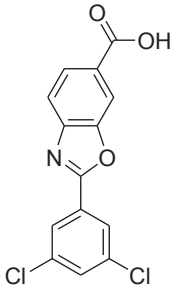

Tafamidis

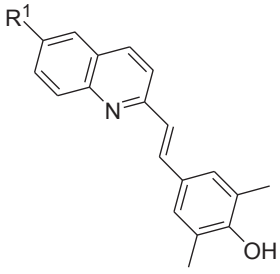

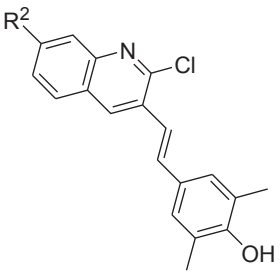

Compound	R^1	R^2	% Fibril Formation (WT-TTR)[a]		IC_{50} (μM)
			7.2 μM	3.6 μM	
Tafamidis			1.0%	14.8%	1.55
10a	H	–	26.3%	–	–
10b	NO_2	–	92.9%	–	–
10c	NH_2	–	26.8%	51.3%	–
14a	–	H	2.3%	33.2%	–
14c	–	OH	0.9%	17.7%	1.49

[a] % Fibril formation represents the extent of more amyloidogenic V30M-TTR fibril formation in the presence of inhibitors (7.2 μM or 3.6 μM inhibitor, 3.6 μM WT-TTR, pH 4.4, 37 °C, 72 h), compared to untreated WT-TTR (100% fibril formation).

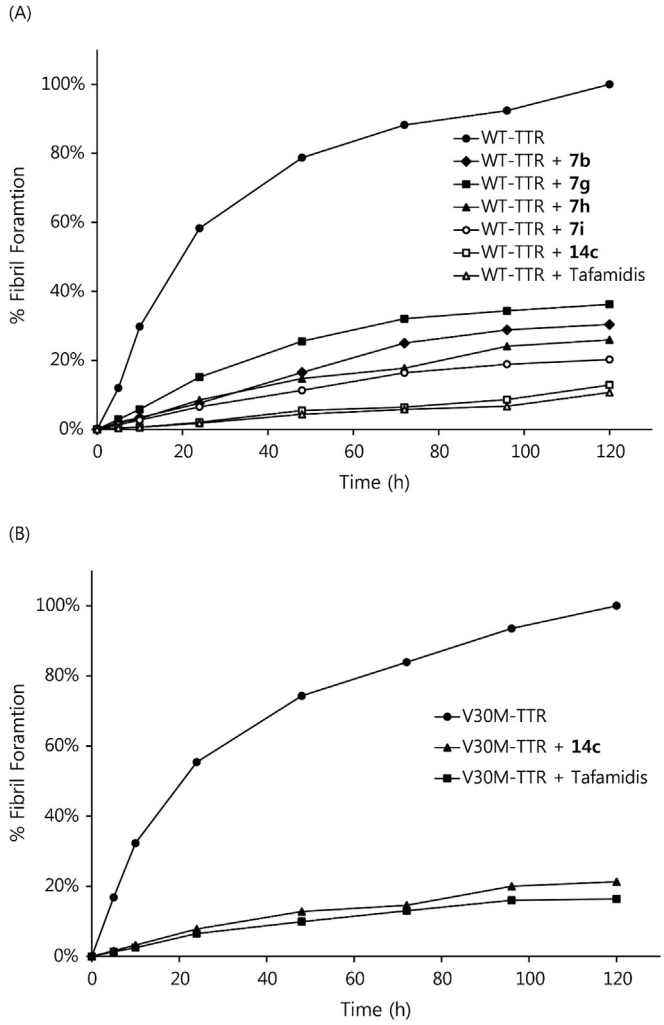

Fig. 2. (A) The time-course of WT-TTR (3.6 μM) fibril formation in the absence and presence of quinoline derivatives and tafamidis (3.6 μM). (B) The time-course of V30M-TTR (3.6 μM) fibril formation in the absence and presence of quinoline derivative **14c** and tafamidis (3.6 μM).

2.2.2. WT- and V30M-TTR aggregation time courses for quinoline derivatives

To further evaluate the potency of selected quinoline derivatives **7b**, **7g**, **7h**, **7i**, and **14c**, the extent of inhibition of acid-mediated WT-TTR fibril formation (pH 4.4) by inhibitors at a concentration equal to the TTR tetramer (3.6 μM) were investigated over a 120 h time course instead of at a fixed time (72 h). As shown in Fig. 2A, the most potent inhibitor **14c** inhibited 7–23% more WT-TTR fibril formation than other inhibitors and significantly showed similar potency to tafamidis. Furthermore, inhibitor **14c** exhibited more than 80% inhibition and significantly suppressed more amyloidogenic V30M-TTR fibril formation (Fig. 2B). Under such an acidic condition, the binding of **14c** to only one T_4 binding site within WT-TTR tetramer was sufficient to kinetically stabilize and to prevent the fibril formation of WT- and V30M-TTR tetramer.

2.3. In silico molecular docking studies

The expected binding mode of compound **14c** with the best activity was displayed in Fig. 3. Atomic coordinates for TTR (PDB ID: 2ROX) were obtained from RCSB protein databank (www.rcsb.org). For compound **14c**, the quinoline-Y ring forms a hydrophobic

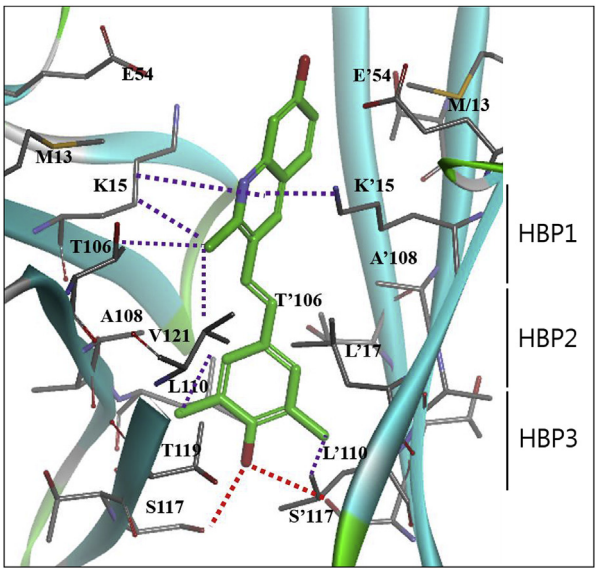

Fig. 3. Docking mode of compound **14c** on the TTR tetramer. The chloride atom of quinoline ring forms the hydrophobic interactions with side chains of K15, T106 and V121 shown in violet lines. As known in 2ROX structure bound with thyroxine, quinolone ring shows the hydrophobic interaction with side chains of K15 and K′15. The hydroxyl group of quinolone ring electrostatically interacts with side chains of E54 and E′54. The hydrogen bond was described in red lines.

interaction with side chains of K15 and K′15, as shown in 2ROX complex structure. The chloride atom of quinolone-Y ring showed the favorable interaction in the hydrophobic cavity formed by side chains of K15, T106 and V121, and thus leading to the activity improvement. Also, the hydroxyl group of quinoline-Y ring was well positioned around the negative side chain of E54 and E′54 showing the favorable electrostatic interaction. Through the hydrophobic channel surrounded by A108, L110, T119, L′17, T′106 and L′110, two methyl group on the aryl-X ring interacts with each hydrophobic residue as shown in Fig. 3, indicated with violet lines. The hydroxyl part of aryl-X ring especially forms the hydrogen bond with side chain of S117 and S′117 described in red lines. The methyl substituents extend into the two symmetry-related halogen binding pockets 3 and 3′. The 4-OH substituent on the aryl-X ring makes bridging hydrogen bonds with the Ser117 and Ser117′ side chains of adjacent TTR subunits.

2.4. In vivo pharmacokinetic profile

Plasma concentration profiles of compounds **7i** and **14c** in fasted male SD rats are shown in the Supplementary Data section. Pharmacokinetic parameters are listed in Table 4. Parameters were calculated for each animal and averaged.

After a single IV injection of 2 mg/kg, the peak plasma concentrations (C_{max}) of **7i** and **14c** in male rats were 3.107 and 2.381 μg/mL, reached at 0.083 h after administration, respectively. The mean systemic plasma clearance (CL) was 1505 and 440.2 mL/h/kg for **7i** and **14c**, respectively. The mean steady state volume of distribution (V_{ss}) for **7i** and **14c** were 1479 and 1128 mL/kg, respectively. Terminal half-life ($T_{1/2}$) was 2.710 and 2.745 h for **7i** and **14c**, respectively. Comparing to hepatic blood flow in rat (3312 mL/h/kg) [42], the CL values of **7i** and **14c** were considered moderate and low, respectively, indicating the elimination rate including metabolism was not high. Meanwhile, V_{ss} values of **7i** and **14c** were moderate, suggesting that **7i** and **14c** were well distributed to tissue in rats.

After a single oral dosing of 5 mg/kg, C_{max} of **7i** and **14c** in male rats was 0.138 and 0.665 μg/mL, reached at 2.450 and 0.598 h after

Table 4
Pharmacokinetic parameters in rats after a single IV and oral administration of **7i** and **14c**.

PK Parameters	**7i**		**14c**	
	IV	Oral	IV	Oral
T_{max} (h)	0.083 ± 0.000	2.450 ± 1.230	0.083 ± 0.000	0.598 ± 0.318
C_{max} (μg/mL)	3.107 ± 0.371	0.138 ± 0.204	2.381 ± 0.358	0.665 ± 0.247
$T_{1/2}$ (h)	2.710 ± 1.059	1.592 ± 0.654	2.745 ± 1.894	3.364 ± 1.428
AUC_{0-t} (μg h/mL)	1.331 ± 0.167	0.226 ± 0.127	4.508 ± 0.557	2.845 ± 0.639
$AUC_{0-\infty}$ (μg h/mL)	1.347 ± 0.170	0.232 ± 0.127	4.590 ± 0.541	3.122 ± 0.698
CL (mL/h/kg)	1505 ± 211.5		440.2 ± 51.30	
V_{ss} (mL/kg)	1479 ± 417		1128 ± 431.2	
BA (%)		6.888 ± 3.761		27.20 ± 6.081

administration, respectively. $T_{1/2}$ for oral dosing of 5 mg/kg was 1.592 and 3.364 h for **7i** and **14c**, respectively. Bioavailability (BA) was estimated by comparing normalized areas under the plasma concentration-time curve ($AUC_{0-\infty}$) for oral and intravenous administration was to be 6.880 and 27.20 for **7i** and **14c**, respectively. Inhibitor **7i** was absorbed slowly and showed low BA value after oral administration. Considering moderate CL value, low BA was not considered to be caused only by low metabolic stability but also by the marginal absorption in intestine. Meanwhile, inhibitor **14c** was absorbed rapidly and showed higher plasma exposure level than **7i**. With moderate BA and low clearance, **14c** was also not considered to be fully absorbed in the rat intestine.

3. Conclusions

We have successfully carried out structure activity relationship studies and identified potent quinoline derivatives, which has the following characteristics as a TTR kinetic stabilizer; aromatic X ring with polar substituents for hydrogen bond interaction and van der Waals interaction, hydrophobic linker L, and aromatic Y ring with polar substituents for electrostatic and/or hydrogen bond interactions. In this study, the focused promising library of quinoline derivatives have been designed by structural optimization by SAR studies and their potency was evaluated by acid-mediated TTR fibril formation. Among these compounds, compounds **7i** and **14c** allowed less than 5% of WT-TTR fibril formation at a concentration equal to the WT-TTR tetramer. The most potent inhibitor **14c** significantly exhibited 80% inhibition against more amyloidogenic V30M-TTR at a concentration equal to the V30M-TTR tetramer over a 120 h time course. In silico docking studies within the T_4 binding sites were carried out to rationalize the binding mode and molecular mechanism for its *anti*-TTR fibril formation activity. From this study, a new class of quinoline derivatives with high potency and good PK properties that could potentially be applied for the treatment of human TTR-related diseases.

4. Experimental section

4.1. Chemistry

4.1.1. General

Unless otherwise indicated, all reactions were run under nitrogen gas. The progress of the reactions was monitored by thin layer chromatography (TLC). All products were determined by ^1H, ^{13}C NMR spectra. ^1H and ^{13}C spectra were recorded on a BRUKER 300 MHz and 600 MHz spectrometer. Chemical shifts are reported relative to internal $CDCl_3$ (Me_4Si, δ 0.0) and DMSO-d_6 (δ 2.50 for ^1H and 39.52 for ^{13}C). All mass spectrometry data were collected by Waters Fraction Lynx MS Autopurification System at the Korea Research Institute of Chemical Technology (KRICT). Final compound purities were determined by analytical reverse phase high performance liquid chromatography (RP-HPLC) performed on a Waters Alience 2695 separation module, using a Waters 2487 dual λ absorbance detector, equipped Alience 2695 autosampler and a Thermo Hypersil Keystone Betabasic-18 column (150 Å pore size, 3 μm particle size, mobile phase A = 0.1% TFA in 99.9% H_2O, mobile phase B = 0.1% TFA in 99.9% MeCN). Linear gradients were run from 100:1 to 0:100 A:B over 25 min.

4.1.2. General procedure for MEM or TIPS protection for compound ***2a-e***

To a solution of compounds **3a-d** (1.0 equiv.) and MEMCl or TIPSCl (1.2 equiv.) in THF was slowly added sodium hydride (60% in mineral oil, 1.1 equiv.) in portion at 0 °C. The solution was allowed to r.t. and stirred for 3–18 h. The solution was quenched with water. The solvent was evaporated and the residue was dissolved with EtOAc. The organic layer was washed with water and brine, and dried with Na_2SO_4. The solution was filtered and concentrated. The crude material was purified by column chromatography (silica gel, Hexane/EtOAc).

*4.1.2.1. 1-Bromo-4-((2-methoxyethoxy)methoxy)benzene (**2a**).* Yield: 94%, ^1H NMR (300 MHz, $CDCl_3$) δ 3.38 (s, 3H), 3.55 (t, J = 4.5 Hz, 2H), 3.82 (t, J = 4.5 Hz, 2H), 5.25 (s, 2H), 6.95 (dd, J = 12 Hz, 2H), 7.38 (dd, J = 9.0 Hz, 2H); ^{13}C NMR (150 MHz, $CDCl_3$) δ 58.44, 67.28, 71.11, 93.04, 113.67, 117.68, 131.82, 155.98.

*4.1.2.2. 5-Bromo-2-((2-methoxyethoxy)methoxy)-1,3-dimethylbenzene (**2b**).* Yield: 94%, ^1H NMR (300 MHz, $CDCl_3$) δ 2.26 (s, 6H), 3.41 (s, 3H), 3.59–3.62 (m, 2H), 3.92–3.95 (m, 2H), 5.03 (s, 2H), 7.15 (s, 2H); ^{13}C NMR (75 MHz, $CDCl_3$) δ 16.71, 59.07, 69.18, 71.75, 97.98, 116.69, 131.38, 133.23, 153.84.

*4.1.2.3. (4-Bromo-2,6-diethylphenoxy)triisopropylsilane (**2c**).* Yield: 77%, ^1H NMR (300 MHz, $CDCl_3$) δ 1.09 (d, J = 7.2 Hz, 18H), 1.19 (t, J = 7.5 Hz, 6H), 2.28 (m, J = 7.2 Hz, 3H), 2.58 (q, J = 7.5 Hz, 4H), 7.10 (s, 2H); ^{13}C NMR (75 MHz, $CDCl_3$) δ 14.16, 14.32, 18.04, 23.42, 113.71, 128.97, 136.27, 151.48.

*4.1.2.4. (4-Bromo-2-ethylphenoxy)triisopropylsilane (**2d**).* Yield: 78%, ^1H NMR (300 MHz, $CDCl_3$) δ 1.10 (d, J = 7.1 Hz, 18H), 1.19 (t, J = 7.6 Hz, 3H), 1.26–1.34 (m, 3H), 2.58 (q, J = 7.5 Hz, 2H), 6.64 (d, J = 8.6 Hz, 1H), 7.12 (dd, J = 2.6, 8.6 Hz, 1H), 7.24 (d, J = 2.6 Hz, 1H); ^{13}C NMR (75 MHz, $CDCl_3$) δ 13.00, 13.95, 18.02, 23.50, 112.77, 119.34, 129.15, 131.91, 136.71, 153.00.

*4.1.2.5. (4-Bromo-2-isopropylphenoxy)triisopropylsilane (**2e**) [43].* Yield: 85%, ^1H NMR (300 MHz, $CDCl_3$) δ 1.10 (d, J = 6.0 Hz, 18H), 1.18 (d, J = 7.5 Hz, 6H), 1.27 (m, J = 6.0 Hz, 3H), 3.30 (m, J = 7.5 Hz, 1H), 6.63 (d, J = 8.6 Hz, 1H), 7.10 (dd, J = 2.6, 8.6 Hz, 1H), 7.27 (d, J = 2.6 Hz, 1H).

*4.1.3. General procedure of the Sonogashira coupling reaction for alkynes **3a-e***

To a solution of compounds **2a-e** (1.0 equiv.), bis(triphenylphosphine)-palladium(II) dichloride (0.1 equiv.), copper(I) iodide (0.1 equiv.) in degassed MeCN was added trimethylsilylacetylene (3–4 equiv.) and Et_3N (3.0 equiv.) and stirred at 66 °C for 3–17 h. The mixture was filtered through Celite and washed with EtOAc. The organic solution was washed with water and brine, and dried with Na_2SO_4. The solution was filtered and concentrated. The crude material was purified by column chromatography (silica gel, Hexane/EtOAc).

*4.1.3.1. (4-(2-Methoxy-ethoxymethoxy)-phenylethynyl)trimethylsilane (**3a**).* Yield: 93%, ^{1}H NMR (300 MHz, $CDCl_3$) δ 0.24 (s, 9H), 3.37 (s, 3H), 3.54 (t, J = 4.5 Hz, 2H), 3.81 (t, J = 4.5 Hz, 2H), 5.27 (s, 2H), 6.97 (d, J = 9.0 Hz, 2H), 7.4 (d, J = 9 Hz, 2H); ^{13}C NMR (150 MHz, $CDCl_3$) δ 0.23, 59.20, 67.94, 71.75, 92.93, 93.43, 105.18, 116.19, 116.67, 133.60, 157.53.

*4.1.3.2. 2((4-((2-methoxyethoxy)methoxy)-3,5-dimethylphenyl)ethynyl)trimethylsilane (**3b**) [34].* Yield: 99%, ^{1}H NMR (400 MHz, $CDCl_3$) δ 0.23 (s, 9H), 2.24 (s, 6H), 3.40 (s, 3H), 3.56–3.62 (m, 2H), 3.90–3.94 (m, 2H), 5.04 (s, 2H), 7.15 (s, 2H).

*4.1.3.3. (2,6-Diethyl-4-((trimethylsilyl)ethynyl)phenoxy)triisopropylsilane (**3c**).* Yield: 54%, ^{1}H NMR (300 MHz, $CDCl_3$) δ 0.25 (s, 9H), 1.08 (d, J = 7.3 Hz, 18H), 1.17 (t, J = 7.5 Hz, 6H), 1.26 (m, 3H), 2.57 (q, J = 7.5 Hz, 4H), 7.16 (s, 2H); ^{13}C NMR (75 MHz, $CDCl_3$) δ 0.12, 14.17, 14.31, 18.02, 23.34, 91.76, 106.10, 115.44, 130.32, 134.18, 153.13.

*4.1.3.4. (2-Ethyl-4-((trimethylsilyl)ethynyl)phenoxy)triisopropylsilane (**3d**).* Yield: 40%, ^{1}H NMR (300 MHz, $CDCl_3$) δ 0.24 (s, 9H), 1.09 (d, J = 7.3 Hz, 18H), 1.16 (t, J = 7.5 Hz, 3H), 1.26–1.33 (m, 3H), 2.60 (q, J = 7.5 Hz, 2H), 6.67 (d, J = 8.3 Hz, 1H), 7.16 (dd, J = 2.0, 8.4 Hz, 1H), 7.28 (d, J = 2.0 Hz, 1H); ^{13}C NMR (75 MHz, DMSO-d_6) δ 0.10, 13.04, 18.01, 23.39, 91.93, 105.75, 115.04, 117.78, 130.62, 133.10, 134.48, 154.47.

*4.1.3.5. (3-Isopropyl-4-(2-methoxy-ethoxymethoxy)phenylethynyl) trimethylsilane (**3e**).* Yield: 61%, ^{1}H NMR (300 MHz, $CDCl_3$) δ 0.25 (s, 9H), 1.10 (d, J = 7.2 Hz, 18H), 1.19 (d, J = 6.9 Hz, 6H), 1.27 (m, J = 6.9 Hz, 3H), 3.33 (m, 1H), 6.67 (d, J = 8.4 Hz, 1H), 7.15 (dd, J = 1.8, 8.4 Hz, 1H), 7.32 (d, J = 1.8 Hz, 1H); ^{13}C NMR (75 MHz, DMSO-d_6) δ 0.11, 13.08, 18.03, 22.62, 26.58, 115.08, 117.78, 117.80, 130.28, 130.39, 130.44, 138.74, 153.82.

*4.1.4. General procedure for the synthesis of terminal alkynes **4a-4e***

To a solution of compounds **3a-e** (1.0 equiv.) in MeOH was added K_2CO_3 (1.0 equiv.) at 0 °C and stirred for 1 h. The reaction mixture was stirred for additional 2.5–5 h at room temperature. The solution was diluted with EtOAc. The solution was washed with water and brine, and dried with Na_2SO_4 and concentrated. The crude material was purified by column chromatography (silica gel, Hexane/EtOAc or Hexane only).

*4.1.4.1. 1-Ethynyl-4-(2-methoxy-ethoxymethoxy)-benzene (**4a**).* Yield: 74%, ^{1}H NMR (300 MHz, $CDCl_3$) δ 3.01 (s, 1H), 3.38 (s, 3H), 3.54–3.57 (m, 2H), 3.81–3.84 (m, 2H), 6.99 (d, J = 8.9 Hz, 2H), 7.41 (d, J = 8.8 Hz, 2H); ^{13}C NMR (75 MHz, $CDCl_3$) δ 58.93, 67.72, 71.50, 76.00, 83.44, 93.20, 115.33, 116.08, 133.48, 157.52.

*4.1.4.2. 5-Ethynyl-2-((2-methoxyethoxy)methoxy)-1,3-dimethylbenzene (**4b**).* Yield: 72%, ^{1}H NMR (300 MHz, $CDCl_3$) δ 2.27 (s, 6H), 2.99 (s, 1H), 3.40 (s, 3H), 3.59–3.62 (m, 2H), 3.93–3.96 (m, 2H), 5.05 (s, 2H), 7.17 (s, 2 H); ^{13}C NMR (75 MHz, $CDCl_3$) δ 16.64, 58.98, 69.10, 71.69, 76.05, 83.48, 97.88, 117.60, 131.19, 132.57, 155.33.

*4.1.4.3. (2,6-Diethyl-4-ethynylphenoxy)triisopropylsilane (**4c**).* Yield: 80%, ^{1}H NMR (300 MHz, $CDCl_3$) δ 1.09 (d, J = 7.4 Hz, 18H), 1.17 (t, J = 7.5 Hz, 6H), 1.27–1.34 (m, 3H), 2.58 (q, J = 7.4 Hz, 4H), 3.00 (s, 1H), 7.18 (s, 2H); ^{13}C NMR (75 MHz, $CDCl_3$) δ 14.14, 14.33, 18.03, 23.30, 75.17, 84.53, 114.44, 130.39, 134.27, 153.28.

*4.1.4.4. (2-Ethyl-4-ethynylphenoxy)triisopropylsilane (**4d**).* Yield: 70%, ^{1}H NMR (300 MHz, $CDCl_3$) δ 1.10 (d, J = 7.2 Hz, 18H), 1.17 (t, J = 7.5 Hz, 3H), 1.25–1.35 (m, 3H), 2.59 (q, J = 7.5 Hz, 2H), 2.99 (s, 1H), 6.70 (d, J = 8.3 Hz, 1H), 7.19 (dd, J = 2.2, 8.2 Hz, 1H), 7.30 (d, J = 2.2 Hz, 1H); ^{13}C NMR (75 MHz, $CDCl_3$) δ 13.03, 18.01, 23.38, 75.30, 84.19, 99.97, 113.95, 117.79, 130.73, 133.18, 134.59, 154.63.

*4.1.4.5. (4-Ethynyl-2-isopropylphenoxy)triisopropylsilane (**4e**).* Yield: 69%, ^{1}H NMR (300 MHz, $CDCl_3$) δ 1.11 (d, J = 7.2 Hz, 18H), 1.19 (d, J = 6.9 Hz, 6H), 1.28–1.35 (m, J = 7.2 Hz, 3H), 2.99 (s, 1H), 3.31 (m, J = 6.9 Hz, 1H), 6.70 (d, J = 8.3 Hz, 1H), 7.17 (dd, J = 2.1, 8.3 Hz, 1H), 7.35 (d, J = 2.1 Hz, 1H); ^{13}C NMR (75 MHz, $CDCl_3$) δ 13.08, 18.04, 22.62, 26.58, 75.23, 84.38, 114.01, 117.81, 130.44, 138.88, 153.98.

*4.1.5. General procedure of Sonogashira coupling reaction for compounds **6a-h***

To a solution of substituted quinolines **5a-d** (1.0 equiv.), ethynylbenzene **4a-e** (1.2–1.4 equiv.), bis(tri-phenylphosphine) palladium(II) dichloride (0.1 equiv.), copper(I) iodide (0.1 equiv.) in degassed Et_3N. The solution was stirred under N_2 at 80 °C for 3–7 h. The mixture was filtered through Celite and washed with EtOAc. The solution was washed with water and brine, and dried with Na_2SO_4. The solution was filtered and concentrated. The crude material was purified by column chromatography (silica gel, Hexane/EtOAc).

*4.1.5.1. 2-((4-((2-Methoxyethoxy)methoxy)phenyl)ethynyl)quinoline (**6a**).* Yield: 97%, ^{1}H NMR (300 MHz, $CDCl_3$) δ 3.37 (s, 3H), 3.55–3.58 (m, 2H), 3.82–3.85 (m, 2H), 5.28 (s, 2H), 7.05 (d, J = 8.8 Hz, 1H), 7.51–7.62 (m, 4H), 7.70–7.76 (m, 1H), 7.79–7.82 (m, 1H), 8.11–8.15 (m, 1H); ^{13}C NMR (75 MHz, $CDCl_3$) δ 59.01, 67.83, 71.54, 88.55, 90.08, 93.24, 115.24, 116.22, 124.30, 126.93, 126.99, 127.46, 129.26, 129.98, 133.77, 136.04, 143.86, 148.22, 157.94.

*4.1.5.2. 2-((4-((2-Methoxyethoxy)methoxy)3,5-dimethylphenyl)ethynyl)quinoline (**6b**).* Yield: 92%, ^{1}H NMR (300 MHz, $CDCl_3$) δ 2.26 (s, 6H), 3.40 (s, 3H), 3.60–3.63 (m, 2H), 3.94–3.97 (m, 2H), 5.09 (s, 2H), 7.35 (s, 2H), 7.51–7.59 (m, 2H), 7.70–7.75 (m, 1H), 7.79 (d, J = 8.0 Hz, 1H), 8.11 (d, J = 8.4 Hz, 2H); ^{13}C NMR (75 MHz, $CDCl_3$) δ 16.82, 59.10, 69.21, 71.77, 88.61, 90.08, 97.98, 117.67, 124.33, 126.95, 127.02, 127.47, 129.30, 129.97, 131.41, 132.86, 136.04, 143.83, 148.24, 155.83.

*4.1.5.3. 2-((3,5-Diethyl-4-(triisopropylsilyloxy)phenyl)ethynyl)quinoline (**6c**).* Yield: 60%, ^{1}H NMR (300 MHz, $CDCl_3$) δ 1.11 (d, J = 7.3 Hz, 18H), 1.21 (t, J = 7.5 Hz, 6H), 1.31 (m, 3H), 2.63 (q, J = 7.5 Hz, 4H), 7.37 (s, 2H), 7.54 (dd, J = 8.1 Hz, 1H), 7.58 (d, J = 8.4 Hz, 1H), 7.70 (dd, J = 8.4 Hz, 1H), 7.79 (d, J = 8.1 Hz, 1H), 8.12 (dd, J = 3.3, 8.4 Hz, 2H); ^{13}C NMR (75 MHz, $CDCl_3$) δ 14.09, 14.37, 18.05, 23.30, 88.17, 91.35, 114.56, 124.32, 126.76, 126.98, 127.45, 129.34, 129.87, 130.65, 134.40, 135.90, 144.24, 148.37, 153.81.

*4.1.5.4. 2-((3-Ethyl-4-(triisopropylsilyloxy)phenyl)ethynyl)quinoline (**6d**).* Yield: 78%, ^{1}H NMR (300 MHz, $CDCl_3$) δ 1.13 (d, J = 7.2 Hz, 18H), 1.21 (t, J = 7.5 Hz, 3H), 1.30 (m, 3H), 2.63 (q, J = 7.5 Hz, 2H), 6.77 (d, J = 8.4 Hz, 1H), 7.37 (dd, J = 2.2, 8.2 Hz, 1H), 7.5–7.56 (m, 2H), 7.58 (d, J = 8.4 Hz, 1H), 7.73 (dd, J = 7.8 Hz, 1H), 7.79 (d, J = 8.2 Hz, 1H), 8.12 (d, J = 8.4 Hz, 2H); ^{13}C NMR (75 MHz, DMSO-d_6)

δ 13.10, 13.93, 18.03, 23.37, 88.26, 91.06, 114.10, 118.00, 124.37, 126.78, 126.99, 127.46, 129.33, 1219.89, 131.01, 133.47, 134.77, 135.92, 144.22, 148.34, 155.17.

*4.1.5.5. 2-((3-Isopropyl-4-(triisopropylsilyloxy)phenyl)ethynyl)quinoline (**6e**).* Yield: 60%, ^{1}H NMR (300 MHz, $CDCl_3$) δ 1.13 (d, J = 7.3 Hz, 18H), 1.23 (d, J = 6.9 Hz, 6H), 1.33 (m, 3H), 3.37 (q, J = 6.9 Hz, 1H), 6.76 (d, J = 8.3 Hz, 1H), 7.35 (dd, J = 2.2, 8.2 Hz, 1H), 7.55 (m, 2H), 7.59 (d, J = 8.5 Hz, 1H), 7.73 (dd, J = 8.0 Hz, 1H), 7.79 (d, J = 7.9 Hz, 1H), 8.12 (d, J = 8.4 Hz, 2H); ^{13}C NMR (75 MHz, $CDCl_3$) δ 13.08, 18.05, 22.69, 26.64, 88.12, 91.20, 114.01, 117.96, 124.35, 126.79, 126.94, 127.46, 129.26, 129.92, 130.69, 130.89, 135.97, 139.05, 144.15, 148.25, 154.48.

*4.1.5.6. 6-Methoxy-2-((4-((2-methoxyethoxy)methoxy)-3,5-dimethylphenyl)ethynyl)quinoline (**6f**).* Yield: 98%, ^{1}H NMR (300 MHz, $CDCl_3$) δ 2.29 (s, 6H), 3.40 (s, 3H), 3.59–3.62 (m, 2H), 3.93–3.96 (m, 5H), 5.08 (s, 2H), 7.04 (d, J = 2.8 Hz, 1H), 7.33 (s, 2H), 7.35–7.39 (dd, J = 9.3, 2.8 Hz, 1H), 7.51 (d, J = 8.5 Hz, 1H), 7.98 (dd, J = 8.4, 3.0 Hz, 2H); ^{13}C NMR (75 MHz, $CDCl_3$) δ 16.78, 53.37, 55.53, 59.06, 69.17, 71.75, 88.63, 89.22, 97.94, 104.98, 117.88, 122.72, 124.63, 128.12, 130.75, 131.32, 132.71, 134.67, 141.18, 144.37, 155.62, 158.16.

*4.1.5.7. 2-((4-((2-Methoxyethoxy)methoxy)-3,5-dimethylphenyl)ethynyl)quinolin-6-ol (**6g**).* Yield: 49%, ^{1}H NMR (300 MHz, $CDCl_3$) δ 2.22 (s, 6H), 3.40 (s, 3H), 3.60–3.62 (m, 2H), 3.92–3.95 (m, 2H), 5.05 (s, 2H), 7.18 (s, 3H), 7.38 (dd, J = 9.1, 2.7 Hz, 1H), 7.49 (d, J = 8.4 Hz, 1H), 7.92 (d, J = 8.5 Hz, 1H), 8.02 (d, J = 9.1 Hz, 1H); ^{13}C NMR (75 MHz, $CDCl_3$) δ 16.72, 59.09, 69.15, 71.74, 87.74, 88.23, 90.15, 97, 91, 109.13, 115.84, 117.57, 122.93, 124.57, 128.56, 130.15, 131.31, 132.66, 134.97, 143.40, 155.66.

*4.1.5.8. 2-((3,5-Dimethyl-4-(triisopropylsilyloxy)phenyl)ethynyl)-6-nitroquinoline (**6h**).* Yield: 40%, ^{1}H NMR (300 MHz, $CDCl_3$) δ 1.13 (d, J = 7.2 Hz, 18H), 1.32 (m, 3H), 2.32 (s, 6H), 7.36 (s, 2H), 7.63 (d, J = 4.7 Hz, 1H), 8.22 (dd, J = 9.1, 2.2 Hz, 1H), 8.49 (d, J = 9.2 Hz, 1H), 9.01 (dd, J = 4.5, 2.5 Hz, 1H), 9.31 (s, 1H); ^{13}C NMR (75 MHz, $CDCl_3$) δ 14.24, 17.75, 17.96, 82.73, 102.62, 113.40, 123.25, 123.27, 124.44, 126.87, 129.06, 131.66, 132.79, 132.95, 145.79, 150.16, 153.15, 155.78.

4.1.6. General procedure of MEM or TIPS deprotection

MEM deprotection: To a solution of MEM protected compound (1.0 equiv.) in MeOH and THF (1:1) was slowly added a catalytic amount of concentrated HCl. The solution was stirred for 4–20 h at room temperature. The solution was diluted with EtOAc. The organic layer was washed with water and brine. The solution was dried with Na_2SO_4. The crude material was purified by reverse column chromatography over C 18 (mobile phase A = 0.1% TFA in H_2O, mobile phase B = 0.1% TFA in MeCN).

TIPS Deprotection: To a solution of TIPS protected compound (1.0 equiv.) in THF was added TBAF (tetra-*n*-butylammonium fluoride, 1 M in THF, 1.7 equiv.).The solution was stirred for 1–2.5 h. The solution was quenched with sat. NH_4Cl. The solution was diluted with EtOAc and washed with water and brine. The solution was dried with Na_2SO_4. The solution was filtered and concentrated. The crude material was purified by column chromatography (silica gel, Hexane/EtOAc).

*4.1.6.1. 4-(Quinolin-2-ylethynyl)phenol (**7a**).* Compound **7a** was prepared according to the general procedure for MEM deprotection reaction. The residue was subjected to reverse column chromatography over C18 (mobile phase A = 0.1% TFA in H_2O, mobile phase B = 0.1% TFA in MeCN). Linear gradients were run from 95%: 5%–60%: 40% (A:B) to give **11a** (95%). ^{1}H NMR (300 MHz, DMSO-d_6) δ 6.84 (d, J = 8.8 Hz, 2H), 7.50 (d, J = 8.7 Hz, 2H), 7.60–7.69 (m, 2H), 7.77–7.83 (m, 1H), 7.98 (d, J = 9.5 Hz, 2H), 8.38 (d, J = 8.4 Hz, 1H), 10.10 (s, 1H); ^{13}C NMR (75 MHz, DMSO-d_6) δ 87.65, 91.39, 111.07, 116.02, 124.25, 126.72, 127.28, 127.85, 128.01, 130.64, 133.86, 137.21, 142.79, 146.98, 159.11; HRMS (ES+) m/z calcd for $C_{17}H_{12}NO$ (MH^+) 246.0919, found 246.0908; Purity: 94%.

*4.1.6.2. 2,6-Dimethyl-4-(quinolin-2-ylethynyl)phenol (**7b**).* Compound **7b** was prepared according to the general procedure for MEM deprotection reaction. The residue was subjected to reverse column chromatography over C18 (mobile phase A = 0.1% TFA in H_2O, mobile phase B = 0.1% TFA in MeCN). Linear gradients were run from 65%: 35%–30%: 70% (A:B) to give **7b** (97%). ^{1}H NMR (300 MHz, DMSO-d_6) δ 2.20 (s, 6H), 7.28 (s, 2H), 7.60–7.67 (m, 2H), 7.78–7.83 (m, 1H), 7.98 (d, J = 8.6 Hz, 2H), 8.38 (d, J = 8.4 Hz, 1H), 8.94 (s, 1H); ^{13}C NMR (75 MHz, DMSO-d_6) δ 16.33, 87.82, 90.73, 111.25, 124.13, 124.92, 126.61, 127.03, 127.89, 128.38, 130.25, 132.13, 136.54, 143.22, 147.60, 155.10; HRMS (ES+) m/z calcd for $C_{19}H_{16}NO$ (MH^+) 274.1232, found 274.1220; Purity: 99%.

*4.1.6.3. 2,6-Diethyl-4-(quinolin-2-ylethynyl)phenol (**7c**).* Compound **7c** was prepared according to the general procedure for TIPS deprotection reaction. The residue was subjected to chromatography (silica gel, Hexane/EtOAc = 5:1) to provide **7c** (64%). ^{1}H NMR (300 MHz, $CDCl_3$) δ 1.29 (t, J = 7.5 Hz, 6H), 2.61 (q, J = 7.5 Hz, 4H), 5.02 (s, 1H), 7.37 (s, 2H), 7.52 (dd, J = 7.5 Hz, 1H), 7.58 (d, J = 8.4 Hz, 1H), 7.71 (dd, J = 7.6 Hz, 1H), 7.80 (d, J = 7.9 Hz, 1H), 8.12 (d, J = 8.5 Hz, 2H); ^{13}C NMR (75 MHz, DMSO-d_6) δ 14.10, 22.68, 87.91, 90.85, 111.68, 124.16, 126.65, 127.05, 127.92, 128.45, 130.27, 130.49, 131.12, 136.51, 143.30, 147.70, 154.07; HRMS (ES+) m/z calcd for $C_{21}H_{20}NO$ (MH^+) 302.1545, found 302.1531; Purity: 99%.

*4.1.6.4. 2-Ethyl-4-(quinolin-2-ylethynyl)phenol (**7d**).* Compound **7d** was prepared according to the general procedure for TIPS deprotection reaction. The residue was subjected to chromatography (silica gel, Hexane/EtOAc = 3:1) to provide **7d** (40%). ^{1}H NMR (300 MHz, $CDCl_3$) δ 1.13 (t, J = 7.5 Hz, 3H), 2.55 (m, 2H), 6.85 (d, J = 8.3 Hz, 1H), 7.33–7.40 (m, 2H), 7.60–7.68 (m, 2H), 7.77 (dd, J = 8.4 Hz, 1H), 7.98 (d, J = 8.3 Hz, 1H), 8.97 (d, J = 8.3 Hz, 2H); ^{13}C NMR (75 MHz, DMSO-d_6) δ 13.76, 22.30, 89.84, 90.64, 111.17, 115.25, 124.05, 126.56, 126.92, 127.81, 128.37, 130.13, 130.75 130.93, 132.76, 136.37, 143.23, 147.63, 156.67; HRMS (ES+) m/z calcd for $C_{19}H_{16}NO$ (MH^+) 274.1232, found 274.1219; Purity: 99%.

*4.1.6.5. 2-Isopropyl-4-(quinolin-2-ylethynyl)phenol (**7e**).* Compound **7e** was prepared according to the general procedure for TIPS deprotection reaction. The residue was subjected to chromatography (silica gel, Hexane/EtOAc = 3:1) to provide **7e** (97%). ^{1}H NMR (300 MHz, $CDCl_3$) δ 1.18 (d, J = 6.9 Hz, 6H), 3.19 (q, J = 6.8 Hz, 1H), 6.86 (d, J = 8.3 Hz, 1H), 7.32 (dd, J = 2.1, 8.2 Hz, 1H), 7.41 (d, J = 2.1 Hz, 1H), 7.62 (dd, J = 6.8 Hz, 1H), 7.67 (d, J = 8.5 Hz, 1H), 7.77–7.83 (m, 1H), 7.98 (d, J = 8.4 Hz, 2H), 8.38 (d, J = 8.5 Hz, 1H); ^{13}C NMR (75 MHz, DMSO-d_6) δ 22.16, 26.20, 89.81, 90.80, 111.26, 115.45, 124.07, 126.57, 126.93, 127.81, 128.36, 130.05, 130.14, 130.68, 135.09, 136.3.7, 143.24, 147.64, 156.10; HRMS (ES+) m/z calcd for $C_{20}H_{18}NO$ (MH^+) 288.1388, found 288.1376; Purity: 99%.

*4.1.6.6. 4-((6-Methoxyquinolin-2-yl)ethynyl)-2,6-dimethylphenol (**7f**).* Compound **7f** was prepared according to the general procedure for MEM deprotection reaction. The residue was subjected to reverse column chromatography over C18 (mobile phase A = 0.1% TFA in H_2O, mobile phase B = 0.1% TFA in MeCN). Linear gradients were run from 85%: 15%–45%: 55% (A:B) to give **7f** (86%). ^{1}H NMR (300 MHz, DMSO-d_6) δ 2.20 (s, 6H), 3.92 (s, 3H), 7.26 (s, 2H), 7.42 (d, J = 2.6 Hz, 1H), 7.45 (dd, J = 9.2, 2.8 Hz, 1H), 7.62 (d,

J = 8.5 Hz, 1H), 7.90 (d, J = 9.0 Hz, 1H), 8.31 (d, J = 8.5 Hz, 1H), 8.93 (s, 1H); ^{13}C NMR (75 MHz, DMSO-d_6) δ 16.38, 55.70, 87.04, 91.68, 105.89, 111.19, 123.41, 124.54, 124.99, 128.08, 128.87, 132.13, 136.37, 139.73, 142.44, 155.22, 157.94; LC/MS (ES+) m/z 303.6 (M^+); Purity: 98%.

*4.1.6.7. 2-((4-Hydroxy-3,5-dimethylphenyl)ethynyl)quinolin-6-ol (**7g**).* Compound **7g** was prepared according to the general procedure for MEM deprotection reaction. The residue was subjected to reverse column chromatography over C18 (mobile phase A = 0.1% TFA in H_2O, mobile phase B = 0.1% TFA in MeCN). Linear gradients were run from 95%: 5%–20%: 80% (A:B) to give **7g** (83%). ^{1}H NMR (300 MHz, DMSO-d_6) δ 2.19 (s, 6H), 7.22–7.25 (m, 3H), 7.40 (dd, J = 9.1, 2.5 Hz, 1H), 7.61 (d, J = 8.6 Hz, 1H), 7.87 (d, J = 9.1 Hz, 1H), 8.30 (d, J = 8.7 Hz, 1H); ^{13}C NMR (75 MHz, DMSO-d_6) δ 16.40, 86.57, 92.55, 108.63, 111.07, 123.82, 124.33, 125.03, 128.27, 128.48, 132.18, 136.56, 138.36, 140.73, 155.34, 156.67; HRMS (ES+) m/z calcd for $C_{19}H_{16}NO_2$ (MH^+) 290.1181, found 290.1169; Purity: 99%.

*4.1.6.8. 2,6-Dimethyl-4-((6-nitroquinolin-2-yl)ethynyl)phenol (**7h**).* Compound **7h** was prepared according to the general procedure for MEM deprotection reaction. The residue was subjected to chromatography over silica gel (Hexane/EtOAc = 3:1) to give **7h** (75%). ^{1}H NMR (300 MHz, DMSO-d_6) δ 2.23 (s, 6H), 7.36 (s, 2H), 7.85 (m, 1H), 8.28 (d, J = 8.9 Hz, 1H), 8.53 (d, J = 9.2 Hz, 1H), 9.11 (s, 2H); ^{13}C NMR (75 MHz, DMSO-d_6) δ 16.37, 82.19, 102.31, 110.71, 122.07, 123.31, 124.56, 125.08, 125.73, 131.19, 131.59, 132.20, 145.43, 149.43, 153.77, 155.73; HRMS (ES+) m/z calcd for $C_{19}H_{15}N_2O_3$ (MH^+) 319.1083, found 319.1070; Purity: 95%.

*4.1.6.9. 4-((6-Aminoquinolin-2-yl)ethynyl)-2,6-dimethylphenol (**7i**).* To a suspension of **7h** (38 mg, 0.119 mmol) in AcOH and HCl (1/0.1 mL, v/v) was added Sn powder (56.7 mg, 0.477 mmol) and stirred for 1 h. The mixture was diluted with EtOAc and neutralized by addition of saturated $NaHCO_3$. The solution was washed with saturated brine and dried with Na_2SO_4. The solution was filtered and concentrated. The residue was subjected to chromatography over silica gel (Hexane/EtOAc = 1:2) to give **7i** (67%). ^{1}H NMR (300 MHz, DMSO-d_6) δ 2.21 (s, 3H), 5.89 (s, 2H), 7.18–7.24 (m, 2H), 7.30 (s, 2H), 7.37 (dd, J = 4.5, 1.6 Hz, 1H), 7.71 (d, J = 8.9 Hz, 1H), 8.42 (dd, J = 4.4, 1.6 Hz, 1H); ^{13}C NMR (75 MHz, DMSO-d_6) δ 16.41, 83.93, 98.65, 102.64, 111.93, 121.95, 122.85, 124.92, 125.21, 129.17, 130.35, 131.94, 141.86, 144.13, 148.04, 154.94; HRMS (ES+) m/z calcd for $C_{19}H_{17}N_2O$ (MH^+) 289.1341, found 289.1328; Purity: 96%.

*4.1.7. General procedure of the Heck coupling reaction for compounds **9a-b***

To a solution of substituted quinolines (**5a-b**) (1.0–1.5 equiv.), compound **8** (1.0 equiv.) in degassed 1,4-dioxane were added $Pd_2(dba)_3$ (0.1–0.2 equiv.), *t*-butylXphos (0.1–0.2 equiv.), and Cy_2NMe (2.0 equiv.). The solution was stirred under N_2 at 120 °C for 18–40 h. The mixture was filtered through Celite and washed with EtOAc. The solution was washed with water and brine, and dried with Na_2SO_4. The crude material was purified by column chromatography (silica gel, Hexane/EtOAc).

*4.1.7.1. (E)-2-(4-((2-Methoxyethoxy)methoxy)-3,5-dimethylstyryl) quinoline (**9a**).* Yield: 24%, ^{1}H NMR (300 MHz, DMSO-d_6) δ 2.28 (s, 6H), 3.26 (s, 3H), 3.50–3.53 (m, 2H), 3.84–3.87 (m, 2H), 5.04 (s, 2H), 7.35 (d, J = 16.3 Hz, 1H), 7.44 (s, 2H), 7.52 (t, J = 7.8 Hz, 1H), 7.71–7.76 (m, 2H), 7.82 (d, J = 8.7 Hz, 1H), 7.92 (t, J = 9 Hz, 2H), 8.32 (d, J = 8.5 Hz, 1H); ^{13}C NMR (75 MHz, DMSO-d_6) δ 13.96, 16.53, 20.62, 58.04, 68.47, 71.12, 97.38, 99.40, 119.74, 125.91, 126.85, 127.62, 127.65, 128.52, 129.64, 130.95, 131.86, 133.56, 136.29, 147.59, 154.96, 155.66.

*4.1.7.2. (E)-2-(4-((2-Methoxyethoxy)methoxy)-3,5-dimethylstyryl)-6-nitro quinoline (**9b**).* Yield: 64%, ^{1}H NMR (300 MHz, DMSO-d_6) δ 2.31 (s, 6H), 3.27 (s, 3H), 3.50–3.53 (m, 2H), 3.84–3.87 (m, 2H), 5.08 (s, 2H), 7.56–7.61 (m, 3H), 7.99 (d, J = 4.7 Hz, 1H), 8.05 (d, J = 16 Hz, 1H), 8.21 (d, J = 9.3 Hz, 1H), 8.48 (dd, J = 2.5, 9.3 Hz, 2H), 9.05 (d, J = 4.7 Hz, 1H), 9.36 (d, J = 2.4, 1H); ^{13}C NMR (75 MHz, DMSO-d_6) δ 16.52, 58.04, 68.51, 71.11, 97.42, 117.99, 120.15, 121.23, 122.58, 124.70, 128.25, 130.94, 131.40, 131.73, 136.58, 144.95, 145.07, 150.29, 153.59, 155.36.

*4.1.7.3. (E)-2,6-Dimethyl-4-(2-(quinolin-2-yl)vinyl)phenol (**10a**).* Compound **10a** was prepared according to the general procedure for MEM deprotection reaction. Yield: 73%. ^{1}H NMR (300 MHz, DMSO-d_6) δ 2.22 (s, 6H), 7.21 (d, J = 16 Hz, 1H), 7.31 (s, 2H), 7.49 (dd, J = 7.4 Hz, 1H), 7.64 (d, J = 16 Hz, 1H), 7.72–7.79 (m, 2H), 7.89–7.96 (m, 2H), 8.27 (d, J = 8.7 Hz, 1H), 8.60 (s, 1H). ^{13}C NMR (75 MHz, DMSO-d_6) δ 17.07, 120.18, 125.08, 125.82, 126.23, 127.29, 127.83, 128.10, 128.20, 129.00, 130.13, 134.96, 136.71, 148.22, 154.84, 156.67; HRMS (ES+) m/z calcd for $C_{19}H_{18}NO$ (MH^+) 276.1388, found 276.1377; Purity: 98%.

*4.1.7.4. (E)-2,6-Dimethyl-4-(2-(6-nitroquinolin-2-yl)vinyl)phenol (**10b**).* Compound **10b** was prepared according to the general procedure for MEM deprotection reaction. Yield: 63%. ^{1}H NMR (300 MHz, DMSO-d_6) δ 2.24 (s, 6H), 7.48 (s, 2H), 7.52 (d, J = 16 Hz, 1H), 7.90 (m, 2H), 8.19 (d, J = 9.3 Hz, 1H), 8.45 (dd, J = 2.4, 9.3 Hz, 1H), 9.01 (d, J = 4.8 Hz, 1H), 9.35 (d, J = 2.3 Hz, 1H); ^{13}C NMR (75 MHz, DMSO-d_6) δ 16.40, 117.40, 117.49, 121.17, 122.44, 124.47, 124.65, 127.19, 128.18, 131.33, 137.35, 144.94, 145.33, 150.35, 153.45, 154.70; HRMS (ES+) m/z calcd for $C_{19}H_{16}N_2O_3$ (MH^+) 321.1239, found 321.1226; Purity: 98%.

*4.1.8. (E)-4-(2-(6-Aminoquinolin-2-yl)vinyl)-2,6-dimethyl phenol (**10c**)*

To a solution of **10b** (150 mg, 0.468 mmol) in EtOH (0.1 M) was added Tin (II) chloride dehydrate ($SnCl_2 \cdot 2H_2O$) (518 mg, 2.295 mmol) and stirred for 9 h at room temperature. The mixture was concentrated and diluted with EtOAc. The organic layer was washed water and brine, and dried with Na_2SO_4. The solution was filtered and concentrated. The crude material was purified by column chromatography (silica gel, Hexane:EtOAc = 1:1) to provide **10c** (83.4 mg, 61%). ^{1}H NMR (300 MHz, DMSO-d_6) δ 2.22 (s, 6H), 5.61 (s, 2H), 7.14 (dd, J = 2.4, 8.9 Hz, 2H), 7.23–7.31 (m, 4H), 7.49–7.55 (m, 2H), 7.68 (d, J = 8.9 Hz, 1H), 8.42 (d, J = 4.7 Hz, 1H), 8.55 (s, 1H); ^{13}C NMR (75 MHz, DMSO-d_6) δ 16.63, 101.14, 116.12, 119.51, 121.21, 124.47, 127.29, 127.67, 127.80, 130.24, 133.43, 139.13, 142.58, 144.67, 147.03, 153.98; HRMS (ES+) m/z calcd for $C_{19}H_{19}N_2O$ (MH^+) 291.1497, found 291.1484; Purity: 96%.

*4.1.9. General procedure of Horner-Wadsworth-Emmons reaction for compounds **13a-b***

To a solution of compound **12** (1.5–2.0 equiv.) in dry DMF (0.1–0.2 M) was added *t*-BuOK (1.5–2.0 equiv.) at 0 °C. The reaction solution was stirred for 10 min. Compound **11a-b** was added to the reaction solution at 0 °C. The solution was stirred for 1–6 h at 60 °C. The solution was diluted with EtOAc. The organic layer was washed with water and brine. The solution was filtered and concentrated. The crude material was purified by column chromatography (silica gel, Hexane:EtOAc).

*4.1.9.1. (E)-2-Chloro-3-(4-((2-methoxyethoxy)methoxy)-3,5-dimethylstyryl)quinoline (**13a**).* Yield:, 43%, ^{1}H NMR (300 MHz, $CDCl_3$) δ 2.36 (s, 6H), 3.43 (s, 3H), 3.62–3.65 (m, 2H), 3.96–4.00 (m, 2H), 5.10 (s, 2H), 7.09 (d, J = 16 Hz, 1H), 7.40 (d, J = 16 Hz, 1H), 7.54–7.59 (m, 1H), 7.68–7.73 (m, 1H), 7.84 (d, J = 8.1 Hz, 1H), 7.99 (d,

J = 8.2 Hz, 1H), 8.36 (s, 1H); ^{13}C NMR (75 MHz, $CDCl_3$) δ 17.02, 59.12, 89.18, 71.80, 77.20, 89.01, 122.46, 127.21, 127.47, 127.55, 127.57, 128.29, 130.06, 130.53, 131.49, 132.48, 132.85, 133.41, 146.70, 155.23.

*4.1.9.2. (E)-2-Chloro-7-methoxy-3-(4-((2-methoxyethoxy)methoxy)-3,5-dimethylstyryl)quinoline (**13b**).* Yield: 55%, ^{1}H NMR (300 MHz,, DMSO-d_6) δ 2.27 (s, 6H), 3.26 (s, 3H), 3.48–3.52 (m, 2H), 3.83–3.86 (m,2H), 3.93 (s, 3H), 5.04 (s, 2H), 7.25–7.38 (m, 6H), 7.03 (d, J = 9.0 Hz, 1H), 8.73 (s, 1H); ^{13}C NMR (75 MHz, $CDCl_3$) δ 16.63, 55.68, 58.13, 68.54, 71.19, 97.46, 106.33, 120.22, 121.67, 122.51, 127.17, 127.20, 129.21, 131.09, 132.04, 132.19, 134.13, 147.92, 149.35, 154.81, 161.14.

*4.1.9.3. (E)-4-(2-(2-Chloroquinolin-3-yl)vinyl)-2,6-dimethyl phenol (**14a**).* Compound **14a** was prepared according to the general procedure for MEM deprotection reaction. The residue was subjected to chromatography (silica gel, Hexane/EtOAc = 5:1) to provide **14a** (68%). ^{1}H NMR (300 MHz, MDSO-d_6) δ 2.21 (s, 6H), 7.22–7.36 (m, 4H), 7.62–7.68 (m, 1H), 7.74–7.79 (m, 1H), 7.91 (d, J = 8.3 Hz, 1H), 8.02 (d, J = 7.3 Hz, 1H), 8.79 (s, 1H); ^{13}C NMR (75 MHz, DMSO-d_6) δ 16.64, 118.91, 124.62, 127.29, 127.44, 127.48, 127.49, 127.53, 127.96, 130.20, 130.28, 133.71, 134.01, 145.78, 149.18, 154.26; HRMS (ES+) m/z calcd for $C_{19}H_{16}ClNO$ (MH^+) 310.0999, found 310.0987; Purity: 99%.

*4.1.9.4. (E)-4-(2-(2-Chloro-7-methoxyquinolin-3-yl)vinyl)-2,6-dimethylphenol (**14b**).* Compound **14b** was prepared according to the general procedure for MEM deprotection reaction. The residue was subjected to chromatography (silica gel, Hexane/EtOAc = 4:1) to provide **14b** (84%). ^{1}H NMR (300 MHz, DMSO-d_6) δ 2.21 (s, 6H), 3.92 (s, 3H), 7.22 (s, 3H), 7.27–7.33 (m, 2H), 7.91 (d, J = 8.9 Hz, 1H), 8.69 (s, 1H); ^{13}C NMR (75 MHz, $CDCl_3$) δ 16.61, 55.64, 106.29, 119.10, 120.13, 122.59, 124.56, 127.06, 127.57, 127.59, 129.08, 132.73, 133.55, 147.65, 149.32, 154.00, 160.93; LC/MS (ES+) m/z 339.6 (M^+); Purity: 94%.

*4.1.10. (E)-2-Chloro-3-(4-hydroxy-3,5-dimethylstyryl) quinolin-7-ol (**14c**)*

To solution of **14b** (20 mg, 0.588 mmol) in DCM was added dropwise BBr_3 (20 μL, 0.206 mmol) at −78 °C. The solution was stirred for 1 h, allowed to r.t. and stirred for 26 h. The solution was quenched with water and diluted with EtOAc. The organic layer was washed with water and brine, and dried with Na_2SO_4. The crude material was purified by column chromatography (silica gel, Hexane/EtOAc = 4:1) to provide **14c** (10.3 mg, 54%). ^{1}H NMR (300 MHz, DMSO-d_6) δ 2.20 (s, 6H), 7.12–7.21 (m, 6H), 7.85 (d, J = 8.9 Hz, 1H), 8.52 (s, 1H), 8.63 (s, 1H); ^{13}C NMR (75 MHz, DMSO-d_6) δ 16.49, 108.84, 119.30, 120.04, 121.70, 124.53, 126.66, 126.91, 127.67, 129.27, 132.16, 133.51, 147.72, 149.21, 153.82, 159.40; HRMS (ES+) m/z calcd for $C_{19}H_{17}ClNO_2$ (MH^+) 326.0948, found 326.0934; Purity: 99%.

4.2. In silico docking study

We carried out a docking study of selected molecules using the released crystal structure complex (PDB ID: 2ROX) [44] of TTR from the RCSB protein databank (www.rcsb.org). The protein was subjected to the "Prepare protein" [45] process using the CHARMm force field and default conditions. Also we built homo-dimer TTR by the homology modeling method of Discovery Studio 4.5 using the symmetry matrix to add other subunits. The prepared homo-dimer structure was then defined as a receptor for the docking calculation. The binding site of TTR was defined as a 15.0 Å sphere around the original ligand of the 2ROX structure. In order to prepare the input molecules, each conformation of the designed molecules was obtained through energy minimization calculations under the CHARMm force field [45]. The designed molecules were docked into the binding site of the TTR by the LibDock [46] protocol of Discovery Studio 4.5.

4.3. Rat pharmacokinetics

Eighteen male SD rats (Orient Bio Inc., Seongnam, Korea) weighing 164–181 g for **7i** and 174–194 g for **14c** were used. Animal room was controlled for illumination (12-h light/dark cycle), temperature (20–25 °C) and relative humidity (>40%). The Institutional Animal Care and Use Committee of the Chungnam National University (Korea) approved the study protocol (license number: CNU-00576).

After overnight fasting, four rats were received an intravenous (IV) dose via tail vein at 2 mg/kg of **7i** or **14c** and five rats were received an oral using gavage needle at 5 mg/kg of **7i** or **14c**. Dosing solution was prepared by dissolving **7i** or **14c** in mixture of 10% DMSO, 40% PEG400 and 50% saline at a concentration of 1 and 2.5 mg/mL for IV and oral, respectively. Blood samples (0.3 mL) were collected from the jugular vein at 0.083 (IV only), 0.25, 0.5, 1, 3, 7, 10 and 24 h after administration.

An aliquot (50 μL) of internal standard (100 ng/mL carbamazepine and 600 ng/mL chlorzoxazone in acetonitrile for **7i** and **14c**, respectively) and 400 μL of acetonitrile were added to an aliquot (50 μL) of plasma to induce precipitation of plasma proteins. This solution was vigorously mixed for 10 min, followed by centrifugation at 12,000 g for 10 min. An aliquot (5 μL) of supernatant was injected into the HPLC/MS/MS system (Agilent 1200 HPLC, Agilent Technologies) which had an API 4000 tandem quadrupole mass spectrometer (Applied Biosystems).

Compounds were separated on Agilent Eclipse Plus® C18 column (3.5 μm, 2.1 × 50 mm) with a gradient of 0.1% formic acid (A) and 0.1% formic acid in acetonitrile (B). For **7i**, the portion of (B) was maintained 50% until 5.0 min. For **14c**, the portion of (B) was maintained 5% until 1.0 min, increased linearly to 95% from 1.0 to 1.5 min, and maintained until 2.5 min. After that, the portion of (B) decreased linearly to 5% from 2.5 to 3.0 min, and maintained until 5 min. A constant flow rate was 0.3 mL/min. A positive multiple reaction monitoring (MRM) mode was used for quantification at m/z 289.236 to 273.300 and 237.198 to 194.200 for **7i** and carbamazepine, respectively. A negative MRM mode was used for quantification at m/z 324.115 to 272.900 and 167.958 to 131.900 for **14c** and chlorzoxazone, respectively. The quantifiable range was from 3 to 3000 ng/mL for **7i** and **14c**. The retention times of **7i**, carbamazepine, **14c** and chlorzoxazone were 3.27, 3.29, 1.84 and 0.77 min, respectively.

The plasma concentration-time profiles were analyzed using moment analysis with WinNonlin 4.1 (Pharsight Corporation).

Acknowledgements

We are grateful for support from the DRC program funded by the National Research Council of Science & Technology (DRC-15-01-KRICT) and Basic Science Research Program through the National Research Foundation of Korea funded by the Ministry of Education, Science and Technology (2015R1D1A3A01020384).

Appendix A. Supplementary data

Supplementary data related to this article can be found at http://dx.doi.org/10.1016/j.ejmech.2016.08.003.

References

[1] F. Chiti, C.M. Dobson, Protein misfolding, functional amyloid, and human

disease, Annu. Rev. Biochem. 75 (2006) 333–366.
[2] C. Soto, Unfolding the role of protein misfolding in neurodegenerative diseases, Nat. Rev. Neurosci. 4 (2003) 49–60.
[3] J.N. Buxbaum, C.E. Tagoe, The genetics of the amyloidoses, Annu. Rev. Med. 51 (2000) 543–569.
[4] J.W. Kelly, W. Colon, Z. Lai, H.A. Lashuel, J. McCulloch, S.L. McCutchen, G.J. Miroy, S.A. Peterson, Transthyretin quaternary and tertiary structural changes facilitate misassembly into amyloid, Adv. Protein Chem. 50 (1997) 161–181.
[5] S.M. Johnson, R.L. Wiseman, Y. Sekijima, N.S. Green, S.L. Adamski-Werner, J.W. Kelly, Native state kinetic stabilization as a strategy to ameliorate protein misfolding diseases: a focus on the transthyretin amyloidoses, Acc. Chem. Res. 38 (2005) 911–921.
[6] Y. Sekijima, R.L. Wiseman, J. Matteson, P. Hammarstrom, S.R. Miller, A.R. Sawkar, W.E. Balch, J.W. Kelly, The biological and chemical basis for tissue selective amyloid disease, Cell 121 (2005) 73–85.
[7] P. Hammarstrom, X. Jiang, A.R. Hurshman, E.T. Powers, J.W. Kelly, Sequence-dependent denaturation energetics: a major determinant in amyloid disease diversity, Proc. Natl. Acad. Sci. U.S.A. 99 (Suppl 4) (2002) 16427–16432.
[8] D.R. Jacobson, R.D. Pastore, R. Yaghoubian, I. Kane, G. Gallo, F.S. Buck, J.N. Buxbaum, Variant-sequence transthyretin (isoleucine 122) in late-onset cardiac amyloidosis in black Americans, N. Engl. J. Med. 336 (1997) 466–473.
[9] Y. Sekijima, P. Hammarstrom, M. Matsumura, Y. Shimizu, M. Iwata, T. Tokuda, S. Ikeda, J.W. Kelly, Energetic characteristics of the new transthyretin variant A25T may explain its atypical central nervous system pathology, Lab. Investig. 83 (2003) 409–417.
[10] P. Hammarstrom, Y. Sekijima, J.T. White, R.L. Wiseman, A. Lim, C.E. Costello, K. Altland, F. Garzuly, H. Budka, J.W. Kelly, D18G transthyretin is monomeric, aggregation prone, and not detectable in plasma and cerebrospinal fluid: a prescription for central nervous system amyloidosis? Biochemistry 42 (2003) 6656–6663.
[11] G.G. Cornwell 3rd, K. Sletten, B. Johansson, P. Westermark, Evidence that the amyloid fibril protein in senile systemic amyloidosis is derived from normal prealbumin, Biochem. Biophys. Res. Commun. 154 (1988) 648–653.
[12] C.C. Blake, M.J. Geisow, S.J. Oatley, B. Rerat, C. Rerat, Structure of prealbumin: secondary, tertiary and quaternary interactions determined by Fourier refinement at 1.8 A, J. Mol. Biol. 121 (1978) 339–356.
[13] H.L. Monaco, M. Rizzi, A. Coda, Structure of a complex of two plasma proteins: transthyretin and retinol-binding protein, Science 268 (1995) 1039–1041.
[14] A. Hornberg, T. Eneqvist, A. Olofsson, E. Lundgren, A.E. Sauer-Eriksson, A comparative analysis of 23 structures of the amyloidogenic protein transthyretin, J. Mol. Biol. 302 (2000) 649–669.
[15] P. Hammarstrom, R.L. Wiseman, E.T. Powers, J.W. Kelly, Prevention of transthyretin amyloid disease by changing protein misfolding energetics, Science 299 (2003) 713–716.
[16] A.R. Hurshman Babbes, E.T. Powers, J.W. Kelly, Quantification of the thermodynamically linked quaternary and tertiary structural stabilities of transthyretin and its disease-associated variants: the relationship between stability and amyloidosis, Biochemistry 47 (2008) 6969–6984.
[17] S. Connelly, S. Choi, S.M. Johnson, J.W. Kelly, I.A. Wilson, Structure-based design of kinetic stabilizers that ameliorate the transthyretin amyloidoses, Curr. Opin. Struc. Biol. 20 (2010) 54–62.
[18] J.C. Sacchettini, J.W. Kelly, Therapeutic strategies for human amyloid diseases, Nat. Rev. Drug Discov. 1 (2002) 267–275.
[19] R.L. Wiseman, S.M. Johnson, M.S. Kelker, T. Foss, I.A. Wilson, J.W. Kelly, Kinetic stabilization of an oligomeric protein by a single ligand binding event, J. Am. Chem. Soc. 127 (2005) 5540–5551.
[20] G.J. Miroy, Z. Lai, H.A. Lashuel, S.A. Peterson, C. Strang, J.W. Kelly, Inhibiting transthyretin amyloid fibril formation via protein stabilization, Proc. Natl. Acad. Sci. U. S. A. 93 (1996) 15051–15056.
[21] S.A. Peterson, T. Klabunde, H.A. Lashuel, H. Purkey, J.C. Sacchettini, J.W. Kelly, Inhibiting transthyretin conformational changes that lead to amyloid fibril formation, Proc. Natl. Acad. Sci. U. S. A. 95 (1998) 12956–12960.
[22] T. Klabunde, H.M. Petrassi, V.B. Oza, P. Raman, J.W. Kelly, J.C. Sacchettini, Rational design of potent human transthyretin amyloid disease inhibitors, Nat. Struct. Biol. 7 (2000) 312–321.
[23] H. Razavi, S.K. Palaninathan, E.T. Powers, R.L. Wiseman, H.E. Purkey, N.N. Mohamedmohaideen, S. Deechongkit, K.P. Chiang, M.T. Dendle, J.C. Sacchettini, J.W. Kelly, Benzoxazoles as transthyretin amyloid fibril inhibitors: synthesis, evaluation, and mechanism of action, Angew. Chem. Int. Ed. Engl. 42 (2003) 2758–2761.
[24] H.M. Petrassi, S.M. Johnson, H. Purkey, K.P. Chiang, T. Walkup, X. Jiang, E.T. Powers, J.W. Kelly, Potent and selective structure-based dibenzofuran inhibitors of transthyretin amyloidogenesis: kinetic stabilization of the native state, J. Am. Chem. Soc. 127 (2005) 6662–6671.
[25] S.M. Johnson, S. Connelly, I.A. Wilson, J.W. Kelly, Biochemical and structural evaluation of highly selective 2-arylbenzoxazole-based transthyretin amyloidogenesis inhibitors, J. Med. Chem. 51 (2008) 260–270.
[26] S.M. Johnson, S. Connelly, I.A. Wilson, J.W. Kelly, Toward optimization of the linker substructure common to transthyretin amyloidogenesis inhibitors using biochemical and structural studies, J. Med. Chem. 51 (2008) 6348–6358.
[27] S.M. Johnson, S. Connelly, I.A. Wilson, J.W. Kelly, Toward optimization of the second aryl substructure common to transthyretin amyloidogenesis inhibitors using biochemical and structural studies, J. Med. Chem. 52 (2009) 1115–1125.
[28] S.M. Johnson, H.M. Petrassi, S.K. Palaninathan, N.N. Mohamedmohaideen, H. Purkey, C. Nichols, K.P. Chiang, T. Walkup, J.C. Sacchettini, K.B. Sharpless, J.W. Kelly, Bisaryloxime ethers as potent inhibitors of transthyretin amyloid fibril formation, J. Med. Chem. 48 (2005) 1576–1587.
[29] V.B. Oza, C. Smith, P. Raman, E.K. Koepf, H.A. Lashuel, H.M. Petrassi, K.P. Chiang, E.T. Powers, J. Sachettinni, J.W. Kelly, Synthesis, structure, and activity of diclofenac analogues as transthyretin amyloid fibril formation inhibitors, J. Med. Chem. 45 (2002) 321–332.
[30] N.S. Green, S.K. Palaninathan, J.C. Sacchettini, J.W. Kelly, Synthesis and characterization of potent bivalent amyloidosis inhibitors that bind prior to transthyretin tetramerization, J. Am. Chem. Soc. 125 (2003) 13404–13414.
[31] S. Choi, S. Connelly, N. Reixach, I.A. Wilson, J.W. Kelly, Chemoselective small molecules that covalently modify one lysine in a non-enzyme protein in plasma, Nat. Chem. Biol. 6 (2010) 133–139.
[32] S. Choi, N. Reixach, S. Connelly, S.M. Johnson, I.A. Wilson, J.W. Kelly, A substructure combination strategy to create potent and selective transthyretin kinetic stabilizers that prevent amyloidogenesis and cytotoxicity, J. Am. Chem. Soc. 132 (2010) 1359–1370.
[33] N.P. Grimster, S. Connelly, A. Baranczak, J. Dong, L.B. Krasnova, K.B. Sharpless, E.T. Powers, I.A. Wilson, J.W. Kelly, Aromatic sulfonyl fluorides covalently kinetically stabilize transthyretin to prevent amyloidogenesis while affording a fluorescent conjugate, J. Am. Chem. Soc. 135 (2013) 5656–5668.
[34] N. Myung, S. Connelly, B. Kim, S.J. Park, I.A. Wilson, J.W. Kelly, S. Choi, Bifunctional coumarin derivatives that inhibit transthyretin amyloidogenesis and serve as fluorescent transthyretin folding sensors, Chem. Commun. 49 (2013) 9188–9190.
[35] E.H. Suh, Y. Liu, S. Connelly, J.C. Genereux, I.A. Wilson, J.W. Kelly, Stilbene vinyl sulfonamides as fluorogenic sensors of and traceless covalent kinetic stabilizers of transthyretin that prevent amyloidogenesis, J. Am. Chem. Soc. 135 (2013) 17869–17880.
[36] S. Gupta, M. Chhibber, S. Sinha, A. Surolia, Design of mechanism-based inhibitors of transthyretin amyloidosis: studies with biphenyl ethers and new structural templates, J. Med. Chem. 50 (2007) 5589–5599.
[37] J. Jung, N. Lee, H. Park, S.J. Park, S. Choi, Design and evaluation of quinolone derivatives as potent inhibitors of wild-type TTR and V30M TTR amyloidogenesis, Bull. Korean Chem. Soc. 36 (2015) 719–722.
[38] T. Coelho, L.F. Maia, A.M. da Silva, M.W. Cruz, V. Plante-Bordeneuve, O.B. Suhr, I. Conceicao, H.H. Schmidt, P. Trigo, J.W. Kelly, R. Labaudiniere, J. Chan, J. Packman, D.R. Grogan, Long-term effects of tafamidis for the treatment of transthyretin familial amyloid polyneuropathy, J. Neurol. 260 (2013) 2802–2814.
[39] T. Coelho, L.F. Maia, A. Martins da Silva, M. Waddington Cruz, V. Plante-Bordeneuve, P. Lozeron, O.B. Suhr, J.M. Campistol, I.M. Conceicao, H.H. Schmidt, P. Trigo, J.W. Kelly, R. Labaudiniere, J. Chan, J. Packman, A. Wilson, D.R. Grogan, Tafamidis for transthyretin familial amyloid polyneuropathy: a randomized, controlled trial, Neurology 79 (2012) 785–792.
[40] C.E. Bulawa, S. Connelly, M. Devit, L. Wang, C. Weigel, J.A. Fleming, J. Packman, E.T. Powers, R.L. Wiseman, T.R. Foss, I.A. Wilson, J.W. Kelly, R. Labaudiniere, Tafamidis, a potent and selective transthyretin kinetic stabilizer that inhibits the amyloid cascade, Proc. Natl. Acad. Sci. U. S. A. 109 (2012) 9629–9634.
[41] Z. Lai, W. Colon, J.W. Kelly, The acid-mediated denaturation pathway of transthyretin yields a conformational intermediate that can self-assemble into amyloid, Biochemistry 35 (1996) 6470–6482.
[42] B. Davies, T. Morris, Physiological-parameters in laboratory-animals and humans, Pharm. Res. 10 (1993) 1093–1095.
[43] N. Takahashi, K. Maeda, Y. Asano, N. Watanabe, Synthesis and pharmacological characterization of 1-benzyl-4-aminoindole-based thyroid hormone receptor β agonists, Bioorg. Med. Chem. 22 (2014) 488–498.
[44] A. Wojtczak, V. Cody, J.R. Luft, W. Pangborn, Structures of human transthyretin complexed with thyroxine at 2.0 A resolution and 3′,5′-dinitro-N-acetyl-L-thyronine at 2.2 A resolution, Acta Crystallogr. D. Biol. Crystallogr. 52 (1996) 758–765.
[45] B.R. Brooks, R.E. Bruccoleri, B.D. Olafson, D.J. States, S. Swaminathan, M. Karplus, CHARMM: a program for macromolecular energy, minimization, and dynamics calculations, J. Comput. Chem. 4 (1983) 187.
[46] D.J. Diller, K.M. Merz, High throughput docking for library design and library prioritization, Proteins 43 (2001) 113–124.